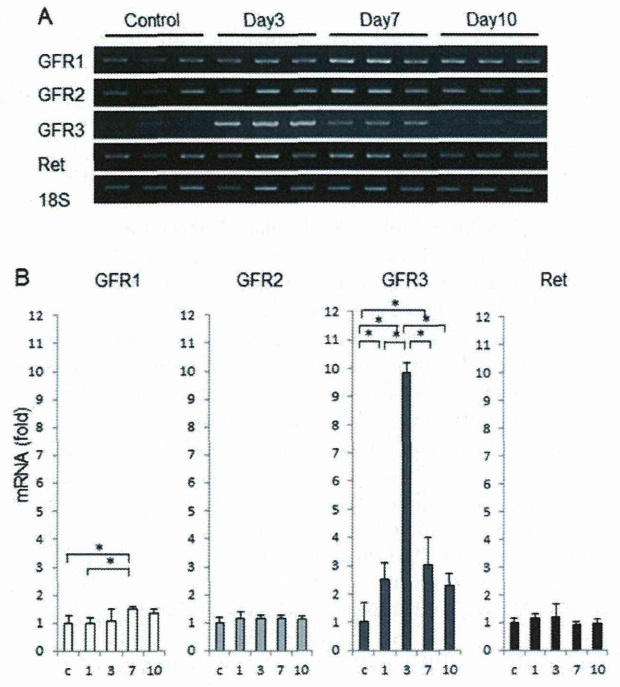

Fig. 1. Changes in expression of mRNA for GDNF-related genes and their receptors on days 3, 7, and 10 after axotomy. **A:** Representative gel images of RT-PCR products. **B:** Quantitative data of real time RT-PCR on days 1, 3, 7, and 10 after axotomy; c, control. $*P < 0.05$.

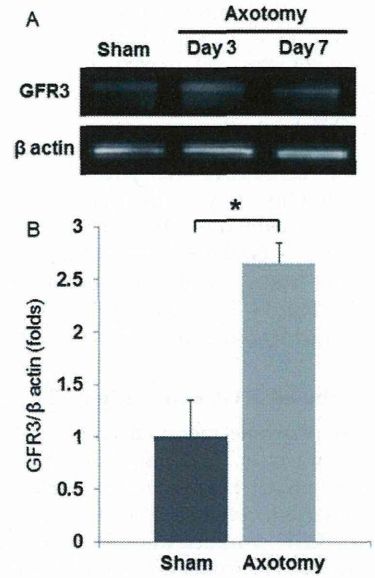

Fig. 2. Changes in expression of protein for GFRα3 on days 3 and 7 after axotomy. **A:** Representative images of immunoblot of sham, day 3, and day7 after axotomy. Upper panel, GFRα3; lower panel, β-actin. **B:** Quantitative data of immune blot of GFRα3/β-actin 3 days after axotomy. $*P < 0.05$.

secondary antibody (1:200, Alexa Fluor-488; Molecular Probes) at RT for 1 hr, and rinsed again with PBS (3 × 5 min). Eight-well chamber slides were mounted with Vectashield mounting medium with DAPI. Controls were stained by omitting the primary antibody. Samples were arranged in a pseudorandomized manner on the plates so that the investigator would not be aware of their identity when quantifying β3-tubulin-positive RGCs. The number of β3-tubulin-positive RGCs was counted in the following manner. Ten random fields per well were captured with a fluorescent microscope (×20 objective) equipped with an imaging system, and the β3-tubulin-positive RGCs were counted in ImageJ. RGCs with axons greater than two RGC diameters in length were defined as RGCs with neurite outgrowths. Values are the mean ± SEM of four replicate wells. Experiments were repeated at least three times. For inhibitor studies, we added U0126, LY294002, SB203829, or JNK2 (Merck-Millipore, Billerica, MA) to the culture medium, and 30 min later ARTN was administered at a final concentration of 1, 10, or 100 ng/ml.

Statistical Analysis

The data from the experimental and control groups were analyzed with ANOVA followed by Scheffé post hoc test in StatView 4.11J software (Abacus Concepts, Berkeley, CA). Statistical analysis for optic nerve regeneration in vivo was performed with the Tukey honest significant difference test. All values were expressed as mean ± standard deviation. $P < 0.05$ was considered statistically significant.

RESULTS

RNA Expression of GFR-Related Genes After Optic Nerve Axotomy

To investigate expressional changes of GFR-related genes after optic nerve axotomy, we performed real-time RT-PCR with several primer sets including GFR-related genes and their coreceptor, Ret. We harvested neural retinas at various time points (control and days 1, 3, 7, and 10) after optic nerve axotomy. Real-time PCR data showed that the expression of GFRα3 increased greater than tenfold 3 days after axotomy ($P < 0.01$; Fig. 1), whereas other members of the GFR family (GFRα1 and GFRα2) were unchanged on day 3. On day 7 after axotomy, the expression of GFRα1 was significantly increased (1.5-fold, $P < 0.05$), and induction of GFRα3 expression was less than on day 3 but still significantly greater than baseline (threefold; $P < 0.05$). On day 10 after axotomy, the expression of all GFR-related genes had returned to control levels. The expression of Ret remained constant during this time period (Fig. 1). We next investigated the protein expression on days 3 and 7 after axotomy. GFRα3 protein had increased significantly by day 3 after axotomy compared with the sham-treated eyes (2.65 ± 0.2-fold, $P < 0.05$; Fig. 2). Immunoblot and immunohistochemistry (IHC) showed that immunoreactivity for GFRα3 antibodies was active in the GCL and inner nuclear layer (INL) and slightly active in the inner plexiform layer (IPL; Fig. 3A). On day 3 after axotomy, immunoreactivity for GFRα3 antibodies was significant

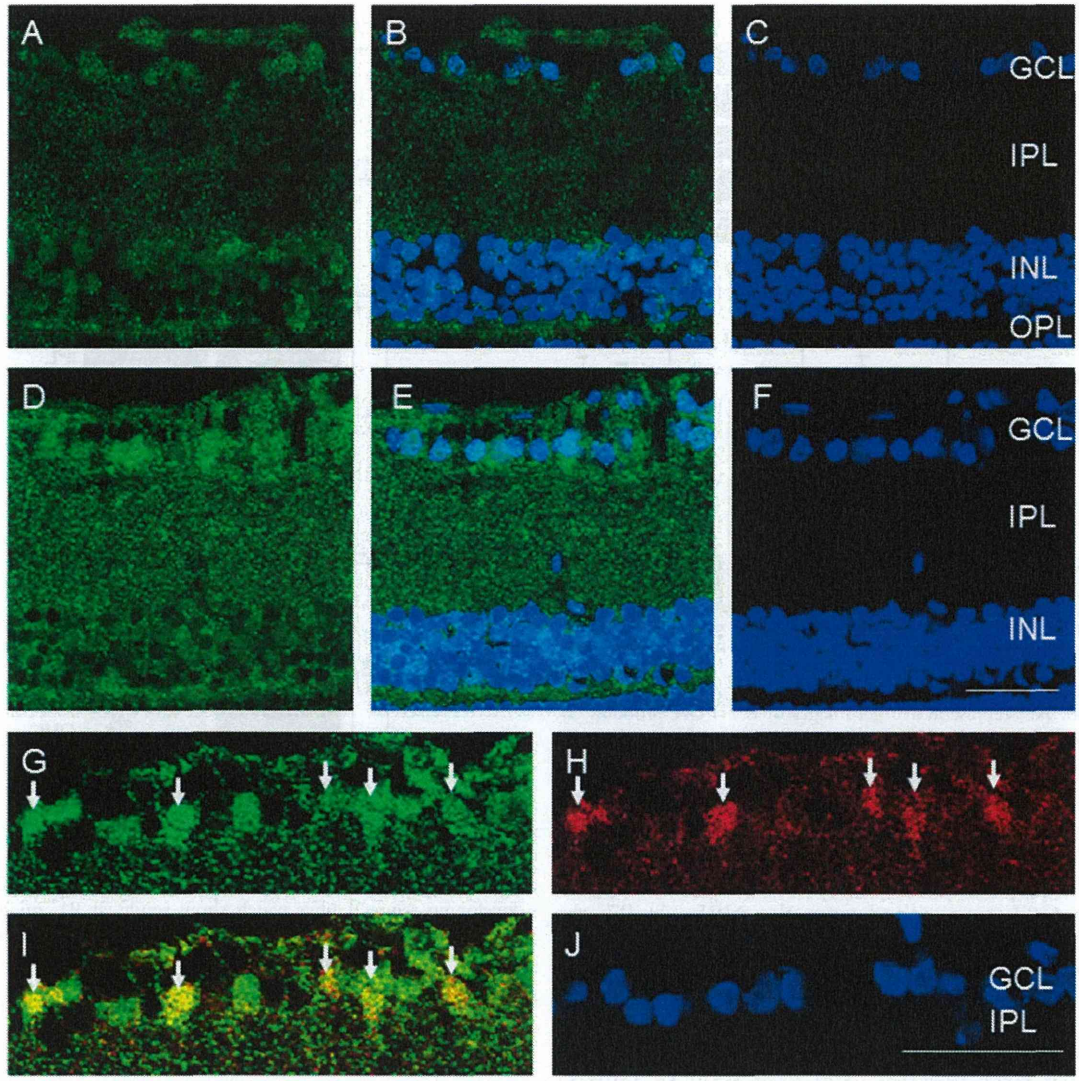

Fig. 3. Representative confocal microscopy photographs of immunohistochemical staining in adult rat retinas with GFRα3 antibodies with or without axotomy. **A–C:** Control retina. **D–J:** Day 3 after axotomy. A,D,G: Immunoreactivity of GFRα3 antibody. B,E,I: Merged images. C,F,J: DAPI nuclear staining. H: Immunoreactivity of Brn3a, an RGC marker. The arrows show RGCs with colocalized GFRα3 and Brn3a. GCL, ganglion cell layer; IPL, inner plexiform layer; INL, inner nuclear layer; OPL, outer plexiform layer. Scale bars = 50 μm.

in the inner retina, including the GCL, IPL, and INL (Fig. 3D). GFRα3 protein was colocalized in the Brn3a-positive RGCs (Fig. 3G–I). These data suggest that GFRα3 is dramatically upregulated following axonal injury at a critical point for RGC survival.

GFRα3 Expression During Retinal Development

Axonal damage can activate neurons' intrinsic axonal growth program, which partially recapitulates an earlier developmental state of neurons (Wang et al., 2007). This possibility prompted us to investigate the expression of GFRα3 and other GFRs during retinal development. Real time RT-PCR showed that the pattern of GFR-family gene expression changed dramatically over the course of retinal development. At embryonic day 14 (E14), the neuroblastic layer (NBL) had just formed (Nakazawa et al., 2000, 2002a), and the expression of GFRα3 stood out among all GFR family members (Fig. 4). At E17, two cellular layers could be distinguished in

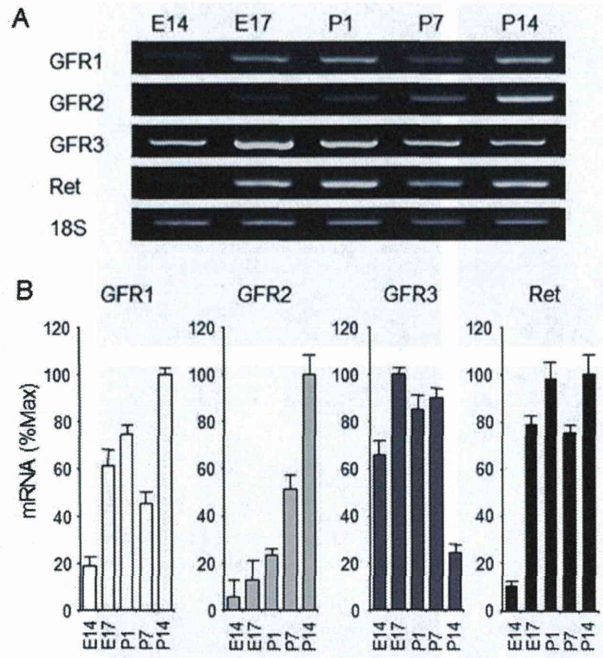

Fig. 4. Developmental profiles of mRNA expression for GDNF-related genes. **A:** Representative gel images of RT-PCR products. **B:** Quantitative data of RT-PCR at E14, E17, P1, P7, and P14. E, embryonic day; P, postnatal day.

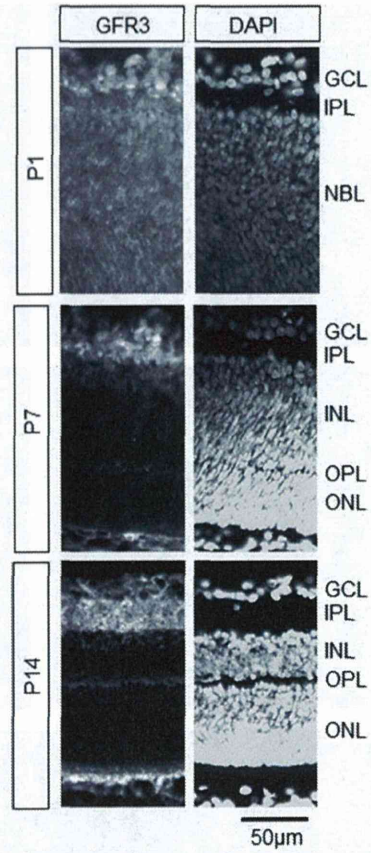

Fig. 5. Immunohistochemical staining with a GFRα3 antibody in the developing retina. Upper panels show results at P1, middle panels at P7, and lower panels at P14 after birth. Left images are IHC for GFRα3 and right images are DAPI nuclear staining. P, postnatal day; GCL, ganglion cell layer; IPL, inner plexiform layer; NBL, neuroblastic layer; INL, inner nuclear layer; OPL, outer plexiform layer; ONL, outer nuclear layer.

the NBL and GFRα1 and GFRα3 were expressed, but GFRα2 expression remained weak. This pattern remained substantially unchanged at postnatal day 1 (P1), when the GCL is separated from the NBL. At P7, the outer plexiform layer (OPL) has formed, and the INL and outer nuclear layer (ONL) can be distinguished. Here, GFRα1 expression decreased and GFRα3 expression remained high, whereas GFRα2 expression began to increase. At P14, retinal layer structure is very similar to adult retinal layer structure, and expression of GFRα1 and GFRα2 increased, whereas the expression of GFRα3 decreased. The expression of Ret was detectable from E17, and the level of Ret mRNA was constant through P14. These data suggest that the expression of GFRα3 is highest in the immature retina and then declines, whereas GFRα1 and GFRα2 are highly expressed in the mature retina. The expression of GFRα3 appears earlier than that of Ret, at E14.

To investigate the distribution of GFRα3 protein in the developing retina further, we performed IHC by using an anti-GFRα3 antibody. At P1, GFRα3 immunoreactivity was detected in the entire retina but was stronger in the cells of the GCL than in the NBL (Fig. 5). At P7, the expression of GFRα3 was strongest in the GCL, IPL, and inner margin of INL. At P14, GFRα3 was detected in the GCL, IPL, inner margin of INL, OPL, and outer segment. These data indicate that, during development, GFRα3 is expressed at its highest levels in the inner retina, including the GCL, IPL, and INL.

Neuroprotective Effect of GFRα3

Next, we investigated the neuroprotective effect of GDNF-family proteins on RGCs in dissociated adult rat primary cultures. We found that GDNF, NRTN, and ARTN all had a neuroprotective effect on adult RGCs at a concentration of more than 10 ng/ml (Fig. 6A–E). To examine the signaling pathway, we treated cells with several pathway inhibitors (U0126 as an MEK inhibitor, LY294002 as a PI3K inhibitor, SB203580 to inhibit p38, and JNK2 to inhibit JNK) in the presence or absence of ARTN (Fig. 6F). Baselines differed with kinase inhibitors in these cultures. Specifically, inhibition of the p38 and JNK pathways had a significant neuroprotective effect on dissociated RGCs in vitro. The quantitative count on the surviving RGCs suggested that the neuroprotective effect of ARTN was suppressed by MAPK and PI3K inhibitors but not by inhibitors of p38 and JNK, suggesting that the neuroprotective effect on cultured RGCs occurs through the MAPK and PI3K signaling pathways.

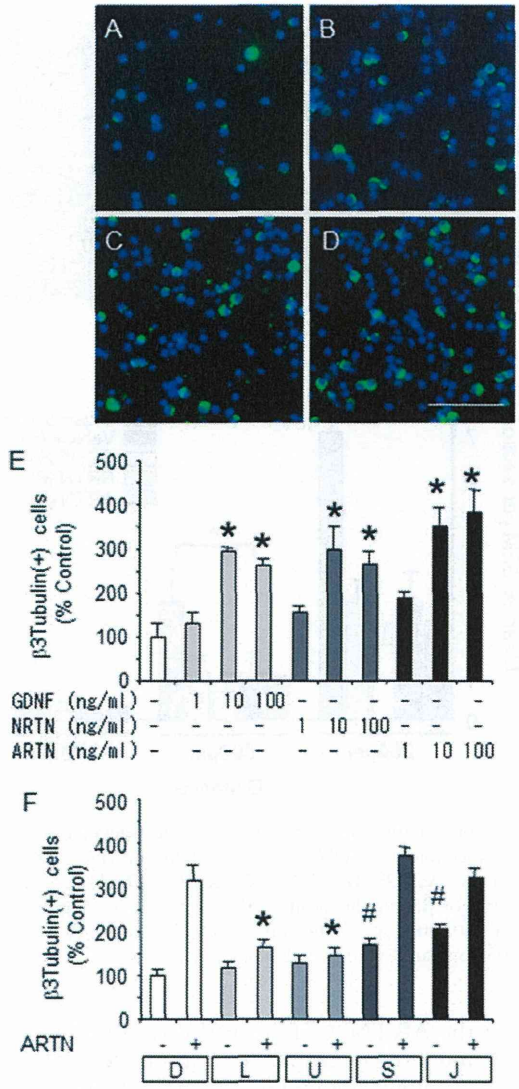

Fig. 6. Representative images of surviving β3-tubulin-positive RGCs following stimulation with GDNF-related proteins in vitro. **A:** PBS. **B:** GDNF. **C:** NTRN. D: ARTN. **E:** Quantitative data of β3-tubulin-positive RGCs with different doses of GDNF-related proteins after 24 hr in vitro. $^{*}P < 0.05$ compared with control without trophic factors. **F:** Quantitative data of β3-tubulin-positive RGCs following treatment with ARTN combined with signaling inhibitors after 24 hr in vitro. D, DMSO; L, LY294002; U, U0126; S, SB203580; J, JNK inhibitor II. $^{*}P < 0.05$ compared with ARTN with DMSO; $^{\#}P < 0.05$ compared with ARTN^{-} condition with DMSO. Scale bar = 50 μm.

To investigate whether GDNF family members have a neuroprotective effect on RGCs, we examined the effects of GDNF, NRTN, and ARTN on the survival of axotomized RGCs in vivo. Ten days after optic nerve damage and intravitreal injection of GDNF family members (1 μg per eye), the retina was harvested, and the density of FG-positive RGCs was counted. The density of

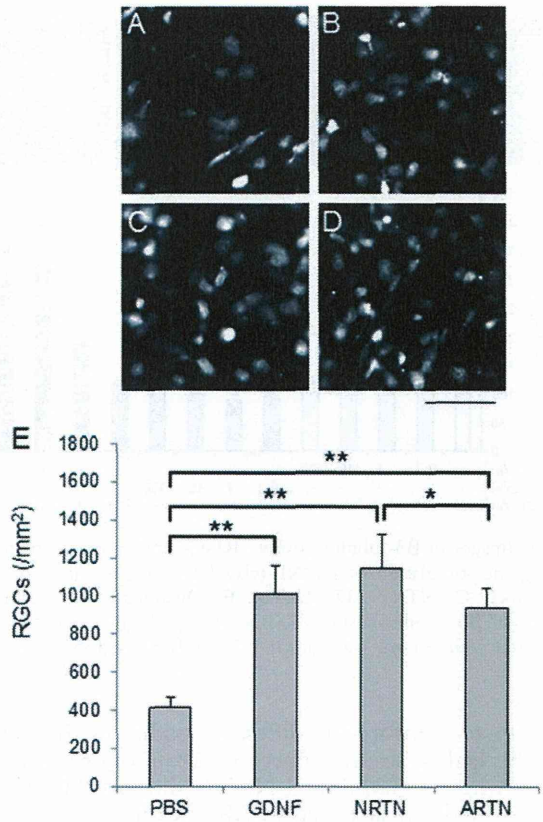

Fig. 7. Representative photographs of FG-labeled RGCs on day 10 after axotomy. **A:** Axotomy with intravitreal administration of PBS. B: GDNF. **C:** NRTN. **D:** ARTN. **E:** Quantitative data of surviving FG-positive RGCs 10 days after axotomy following treatment with PBS, GDNF, NTRN, and ARTN. $^{*}P < 0.05$, $^{**}P < 0.01$. Scale bar = 100 μm.

FG-labeled RGCs was found to be 415 ± 50 cells/mm^2 after injecting PBS (n = 10), 1,013 ± 150 with GDNF (n = 10; $P < 0.0001$), 1,143 ± 150 with NRTN (n = 10, $P < 0.0001$), and 935 ± 107 with ARTN (n = 10, $P = 0.001$; Fig. 7). There was a significant difference between NRTN and ARTN ($P = 0.045$). These data suggest that GDNF family proteins have a neuroprotective effect on axotomized RGCs.

Effect of Axonal Regeneration in Vivo and in Vitro

At E14, developing RGCs extend their axons toward the brain, and expression of GFRα3 is much higher than GFRα1 and GFRα2 at this time point. This developmental profile of GFRα3 led us to investigate the effect of ARTN on axonal growth after injury in adult animals. No significant differences were found in surviving RGCs after 72 hr in vitro with antioxidants and treatment with PBS (40.3 ± 6.6 cells per field; CPF), GDNF (52.4 ± 9.4 CPF), NRTN (58.3 ± 7.9 CPF), or ARTN (54.7 ± 12.0 CPF). Therefore, we showed the percentage

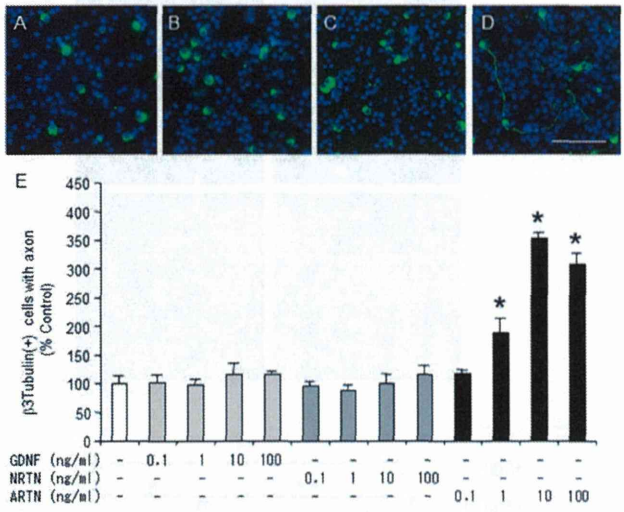

Fig. 8. Images of β3-tubulin-positive RGCs with axonal growth following the stimulation of GDNF-related proteins in vitro. **A:** PBS. **B:** GDNF. **C:** NTRN. **D:** ARTN. **E:** Quantitative data of axonal growth in β3-tubulin-positive RGCs after 72 hr in vitro. $\star P < 0.05$ compared with control without GDNF family protein. Scale bar = 50 μm.

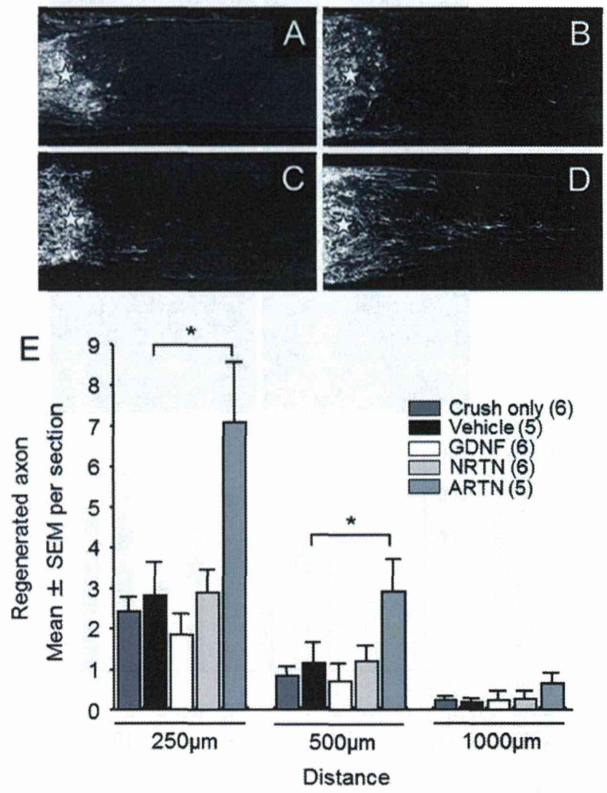

Fig. 9. Representative photographs of axonal regeneration following multiple injections of GDNF-related proteins in vivo. Stars indicate the crush site. **A:** PBS. **B:** GDNF. **C:** NTRN. **D:** ARTN. **E:** Quantitative data of β3-tubulin-positive RGCs with axonal growth at distances of 250, 500, and 1,000 μm on day 21 after optic nerve crush. $\star P < 0.05$ compared with vehicle control in the same points.

in order to compare the different conditions. In culture, ARTN had a strong effect on axon outgrowth after 72 hr, whereas GDNF and NRTN did not (Fig. 8). We also detected similar effects of ARTN on axonal regeneration in vivo with multiple administrations (Fig. 9). These results indicate that, among GDNF family members, ARTN and its receptor GFRα3 have a unique effect on axonal growth of RGCs.

DISCUSSION

This study demonstrates that optic nerve injury induces the upregulation of GFRα3 within 3 days, a critical time point for determining the fate of injured RGCs. To gain insight into the role of GFRα3 after axotomy, we investigated its expression during retinal development and found that, among GDNF family members, the expression of GFRα3 was particularly high throughout embryonic development and in the early postnatal period, then gradually decreased at later stages of maturation. Profiles of GFRα1 and GFRα2 expression were very different from that of GFRα3, suggesting substantial differences in the roles of different GFR family members during development. To examine the role of GFRα3 further, we assessed the effects of ARTN on RGC survival and axon regeneration both in vivo and in vitro. All of the GDNF family members (GDNF, NRTN, and ARTN) had neuroprotective effects on axotomized RGCs. Investigation of intracellular signaling pathways suggested that the neuroprotective effect of ARTN was through the MAPK and PI3K signaling pathways. However, among GDNF family members, ARTN alone stimulated the regrowth of RGC axons both in vivo and in vitro. These findings suggest that the ARTN–GFRα3 pathway contributes to the survival and axonal growth of axotomized RGCs in a way that is unique among GDNF family members.

The present study indicates that both GDNF and NRTN had a neuroprotective effect on axotomized RGCs. This is in agreement with the findings of previous studies that used RGC injury models (Koeberle and Ball, 2002; Ozden and Isenmann, 2004; Ward et al., 2007). Here, we also report for the first time that ARTN had a neuroprotective effect on axotomized RGCs. The neuroprotective effect of NRTN was strongest among GDNF family members, whereas the neuroprotective effect of ARTN was weaker than that of the other members. One possibility is that the roles of ARTN and GFRα3 might differ in RGC survival and axonal growth.

Seventy-two hours after axotomy, the expression of GFRα3, the embryonically dominant form of the GFR family, was significantly upregulated. Previously, we had shown that RB3, a tubulin disassembly factor, is also upregulated in the GCL and peaks at 3 days after optic nerve axotomy (Nakazawa et al., 2005a). Tubulin remodeling is a critical step for axonal growth. Furthermore,

microarray analysis with axotomized purified RGCs shows that significant changes in gene expression are an essential aspect of the growth phase of axotomized RGCs (Fischer et al., 2004). These data suggest that 3 days after axotomy is a critical time point for determining the fate of RGCs.

The effect of GDNF on axonal growth was previously reported to be weak in vitro (Yin et al., 2003), and, in agreement with this finding, we found that GDNF and NRTN have no effects on axonal growth. Unlike GDNF and NRTN, ARTN promotes axonal growth in mature RGCs and might play a similar role in development, as suggested by the high levels of GFRα3 expression during development and in the early postnatal period when RGCs are forming their connections and decline in maturity. ARTN has also been shown to activate axonal growth in the mature DRG via SFK- and extracellular signal-related kinase-dependent signaling pathways (Jeong et al., 2008). Like ARTN, Bcl-2-associated athanogene-1 has been reported to have dual effects on neuroprotection and axonal growth in axotomized RGCs, inducing a translocation of Raf-1 and ROCK2 and interaction with the inhibitory ROCK signaling cascade, which results in dual effects on the prevention of apoptosis and axonal regrowth (Planchamp et al., 2008). Phosphotase and tensin homolog gene deletion also stimulates both RGC survival and axon regeneration after axotomy. (Park et al., 2008) Thus, although several factors have been reported to stimulate axon outgrowth alone (oncomodulin; Kurimoto et al., 2010) or survival alone (e.g., bcl2 overexpression [Chierzi et al., 1999], GDNF [this study], and BDNF [Pernet and Di Polo, 2006]), ARTN is among the factors that stimulate both cell survival and axonal growth. In conclusion, we have demonstrated that increased expression of GFRα3 and ARTN stimulate axonal growth both in vivo and in vitro. Additional study using anti-ARTN antibodies, a specific inhibitor of GFRα3, or GFRα3-deficient mice will be required to conclude that this pathway was critical for axon regeneration after nerve crush. However, the GFRα3-dependent pathway may be an attractive target to stimulate the survival and regenerative capacity of RGCs following optic nerve injury.

ACKNOWLEDGMENTS

The authors thank Prof. Larry Benowitz for important comment and discussion, Mrs. Junko Sato for technical assistance, and Mr. Tim Hilts for editing the manuscript.

REFERENCES

Baloh RH, Enomoto H, Johnson EM Jr, Milbrandt J. 2000. The GDNF family ligands and receptors: implications for neural development. Curr Opin Neurobiol 10:103–110.

Brantley MA Jr, Jain S, Barr EE, Johnson EM Jr, Milbrandt J. 2008. Neurturin-mediated ret activation is required for retinal function. J Neurosci 28:4123–4135.

Carmillo P, Dago L, Day ES, Worley DS, Rossomando A, Walus L, Orozco O, Buckley C, Miller S, Tse A, Cate RL, Rosenblad C, Sah DW, Gronborg M, Whitty A. 2005. Glial cell line-derived neurotrophic factor (GDNF) receptor alpha-1 (GFR alpha 1) is highly selective for GDNF versus artemin. Biochemistry 44:2545–2554.

Chierzi S, Strettoi E, Cenni MC, Maffei L. 1999. Optic nerve crush: axonal responses in wild-type and bcl-2 transgenic mice. J Neurosci 19: 8367–8376.

Fischer D, Petkova V, Thanos S, Benowitz LI. 2004. Switching mature retinal ganglion cells to a robust growth state in vivo: gene expression and synergy with RhoA inactivation. J Neurosci 24:8726–8740.

Hauck SM, Kinkl N, Deeg CA, Swiatek-de Lange M, Schoffmann S, Ueffing M. 2006. GDNF family ligands trigger indirect neuroprotective signaling in retinal glial cells. Mol Cell Biol 26:2746–2757.

Jeong DG, Park WK, Park S. 2008. Artemin activates axonal growth via SFK- and ERK-dependent signalling pathways in mature dorsal root ganglia neurons. Cell Biochem Funct 26:210–220.

Koeberle PD, Bahr M. 2008. The upregulation of GLAST-1 is an indirect antiapoptotic mechanism of GDNF and neurturin in the adult CNS. Cell Death Differ 15:471–483.

Koeberle PD, Ball AK. 2002. Neurturin enhances the survival of axotomized retinal ganglion cells in vivo: combined effects with glial cell line-derived neurotrophic factor and brain-derived neurotrophic factor. Neuroscience 110:555–567.

Kurimoto T, Ishii M, Tagami Y, Nishimura M, Miyoshi T, Tsukamoto Y, Mimura O. 2006. Xylazine promotes axonal regeneration in the crushed optic nerve of adult rats. Neuroreport 17:1525–1529.

Kurimoto T, Yin Y, Omura K, Gilbert HY, Kim D, Cen LP, Moko L, Kugler S, Benowitz LI. 2010. Long-distance axon regeneration in the mature optic nerve: contributions of oncomodulin, cAMP, and pten gene deletion. J Neurosci 30:15654–15663.

Lin LF, Doherty DH, Lile JD, Bektesh S, Collins F. 1993. GDNF: a glial cell line-derived neurotrophic factor for midbrain dopaminergic neurons. Science 260:1130–1132.

Lindahl M, Timmusk T, Rossi J, Saarma M, Airaksinen MS. 2000. Expression and alternative splicing of mouse Gfra4 suggest roles in endocrine cell development. Mol Cell Neurosci 15:522–533.

Nakazawa T, Nakano I, Furuyama T, Morii H, Tamai M, Mori N. 2000. The SCG10-related gene family in the developing rat retina: persistent expression of SCLIP and stathmin in mature ganglion cell layer. Brain Res 861:399–407.

Nakazawa T, Nakano I, Sato M, Nakamura T, Tamai M, Mori N. 2002a. Comparative expression profiles of Trk receptors and Shc-related phosphotyrosine adapters during retinal development: potential roles of N-Shc/ShcC in brain-derived neurotrophic factor signal transduction and modulation. J Neurosci Res 68:668–680.

Nakazawa T, Tamai M, Mori N. 2002b. Brain-derived neurotrophic factor prevents axotomized retinal ganglion cell death through MAPK and PI3K signaling pathways. Invest Ophthalmol Vis Sci 43:3319–3326.

Nakazawa T, Shimura M, Tomita H, Akiyama H, Yoshioka Y, Kudou H, Tamai M. 2003. Intrinsic activation of PI3K/Akt signaling pathway and its neuroprotective effect against retinal injury. Curr Eye Res 26:55–63.

Nakazawa T, Morii H, Tamai M, Mori N. 2005a. Selective upregulation of RB3/stathmin4 by ciliary neurotrophic factor following optic nerve axotomy. Brain Res 861:399–407.

Nakazawa T, Shimura M, Endo S, Takahashi H, Mori N, Tamai M. 2005b. N-methyl-D-aspartic acid suppresses Akt activity through protein phosphatase in retinal ganglion cells. Mol Vis 11:1173–1182.

Nakazawa T, Takahashi H, Nishijima K, Shimura M, Fuse N, Tamai M, Hafezi-Moghadam A, Nishida K. 2007. Pitavastatin prevents NMDA-induced retinal ganglion cell death by suppressing leukocyte recruitment. J Neurochem 100:1018–1031.

Ozden S, Isenmann S. 2004. Neuroprotective properties of different anesthetics on axotomized rat retinal ganglion cells in vivo. J Neurotrauma 21:73–82.

Park KK, Liu K, Hu Y, Smith PD, Wang C, Cai B, Xu B, Connolly L, Kramvis I, Sahin M, He Z. 2008. Promoting axon regeneration in the adult CNS by modulation of the PTEN/mTOR pathway. Science 322:963–966.

Pernet V, Di Polo A. 2006. Synergistic action of brain-derived neurotrophic factor and lens injury promotes retinal ganglion cell survival but leads to optic nerve dystrophy in vivo. Brain 129:1014–1026.

Planchamp V, Bermel C, Tonges L, Ostendorf T, Kugler S, Reed JC, Kermer P, Bahr M, Lingor P. 2008. BAG1 promotes axonal outgrowth and regeneration in vivo via Raf-1 and reduction of ROCK activity. Brain 131:2606–2619.

Sariola H, Saarma M. 2003. Novel functions and signalling pathways for GDNF. J Cell Sci 116:3855–3862.

Trupp M, Scott R, Whittemore SR, Ibanez CF. 1999. Ret-dependent and -independent mechanisms of glial cell line-derived neurotrophic factor signaling in neuronal cells. J Biol Chem 274:20885–20894.

Wang JT, Kunzevitzky NJ, Dugas JC, Cameron M, Barres BA, Goldberg JL. 2007. Disease gene candidates revealed by expression profiling of retinal ganglion cell development. J Neurosci 27:8593–8603.

Ward MS, Khoobehi A, Lavik EB, Langer R, Young MJ. 2007. Neuroprotection of retinal ganglion cells in DBA/2J mice with GDNF-loaded biodegradable microspheres. J Pharm Sci 96:558–568.

Worby CA, Vega QC, Chao HH, Seasholtz AF, Thompson RC, Dixon JE. 1998. Identification and characterization of GFRalpha-3, a novel coreceptor belonging to the glial cell line-derived neurotrophic receptor family. J Biol Chem 273:3502–3508.

Yin Y, Cui Q, Li Y, Irwin N, Fischer D, Harvey AR, Benowitz LI. 2003. Macrophage-derived factors stimulate optic nerve regeneration. J Neurosci 23:2284–2293.

Yin Y, Henzl MT, Lorber B, Nakazawa T, Thomas TT, Jiang F, Langer R, Benowitz LI. 2006. Oncomodulin is a macrophage-derived signal for axon regeneration in retinal ganglion cells. Nat Neurosci 9:843–852.

Clinical Ophthalmology

Dovepress
open access to scientific and medical research

Open Access Full Text Article

ORIGINAL RESEARCH

The effect of intravitreal bevacizumab on ocular blood flow in diabetic retinopathy and branch retinal vein occlusion as measured by laser speckle flowgraphy

Fumihiko Nitta[1]
Hiroshi Kunikata[1,2]
Naoko Aizawa[1]
Kazuko Omodaka[1]
Yukihiro Shiga[1]
Masayuki Yasuda[1]
Toru Nakazawa[1–3]

[1]Department of Ophthalmology, Tohoku University Graduate School of Medicine, Sendai, Japan; [2]Department of Retinal Disease Control, Tohoku University Graduate School of Medicine, Sendai, Japan; [3]Department of Advanced Ophthalmic Medicine, Tohoku University Graduate School of Medicine, Sendai, Japan

Background: This study evaluated the effect of intravitreal injection of bevacizumab (IVB) on macular edema associated with diabetic retinopathy (DME) or branch retinal vein occlusion (BRVOME) using laser speckle flowgraphy.

Methods: A comparative interventional study of 25 eyes from 22 patients with macular edema (DME group: 12 eyes; BRVOME group: 13 eyes) who underwent IVB. Mean blur rate (MBR) was measured in the retinal artery, retinal vein, optic nerve head (ONH), and choroid before and after IVB.

Results: In the BRVOME group, there was no significant change in MBR in the retinal artery, retinal vein or ONH, but choroidal MBR decreased significantly (P=0.04). In the DME group, the MBR in the retinal artery, retinal vein, ONH, and choroid decreased significantly (P=0.02, P=0.04, P<0.001, and P=0.04, respectively). In the DME group, pre-IVB MBR in the ONH was significantly correlated with post-IVB foveal thickness (R= −0.71, P=0.002). There was no such correlation in the BRVOME group in the ONH.

Conclusion: IVB had a suppressive effect on circulation in eyes with DME but not in those with BRVOME. This suggests that this noninvasive and objective biomarker may be a useful part of pre-IVB evaluations and decision-making in DME.

Keywords: macular edema, mean blur rate, optic nerve head, biomarker, ocular circulation

Introduction

Macular edema is one of the main causes of reduced vision in various retinal diseases, including diabetic retinopathy (DR) and branch retinal vein occlusion (BRVO).[1–4] This condition is difficult to treat successfully, even for experienced ophthalmologists. Currently, intravitreal injection of bevacizumab (IVB), an anti-vascular endothelial growth factor (VEGF) antibody, is one of the most accepted treatments.[5–8] It can improve vision by temporarily blocking VEGF action and subsequently reducing macular edema. However, in cases of DR- or BRVO-associated macular edema (DME and BRVOME, respectively), the effect of IVB is often insufficient, requiring the treatment to be repeated many times.[8–11] It is not known why the effectiveness of the treatment is poor in these cases, as the underlying mechanism of IVB's ability to reduce macular edema is still not well understood. Furthermore, the effect of IVB on retinal circulation is also unknown, although there are a few reports that IVB causes a decrease in intraocular and systemic circulation.[12,13] Particularly, IVB can adversely affect the visual prognosis of patients with central retinal vein occlusion and underlying systemic diseases such as diabetes, or ischemic heart or cerebrovascular diseases.[14,15]

Correspondence: Hiroshi Kunikata
Department of Ophthalmology, Tohoku University Graduate School of Medicine, 1-1 Seiryo-machi, Aoba-ku, Sendai 980-8574, Japan
Tel +81 22 717 7294
Fax +81 22 717 7298
Email kunikata@oph.med.tohoku.ac.jp

submit your manuscript | www.dovepress.com
Dovepress
http://dx.doi.org/10.2147/OPTH.S62022

Ischemic change after any medical intervention is ordinarily evaluated with fluorescein angiography, but this technique is invasive, can cause severe complications, including anaphylactic shock, and its results can be affected by time-dependent changes after injection. Recent innovations in an alternative technique, laser speckle flowgraphy (LSFG), have allowed us to quickly and easily monitor changes in tissue circulation over time.[16,17] The main measurement parameter of LSFG, mean blur rate (MBR), is an automatically calculated index of ocular blood flow derived from the scatter pattern produced when the ocular fundus is irradiated with laser light. MBR represents the velocity of the blurring in the speckle pattern that is caused by blood flow. Measured values of MBR correlate well with absolute blood flow values measured with the hydrogen gas clearance and microsphere methods.[18,19] Previous reports have shown that despite being a relative value, MBR can be considered an accurate representation of both ocular blood flow and velocity.[20,21] The quality of LSFG measurements mainly relies on the clarity of the ocular media, but LSFG has already contributed to many recent findings in glaucoma research, and is especially useful in examining the relationship between glaucoma and ocular circulation.[16,22–25]

In this study, we hypothesized that IVB had a different effect on ocular blood circulation in DME and BRVOME. We evaluated the association between MBR and clinical findings in post-IVB eyes in order to reveal the different pathogenesis of DME and BRVOME, and to find new biomarkers of post-IVB visual prognosis. Thus, our purpose was to evaluate the effect of IVB in DME and BRVOME patients by examining the association of MBR and clinical findings related to the structure and function of the retina.

Materials and methods

Setting and design

This was an institutional, prospective, nonrandomized, interventional case series. Subjects were recruited from patients referred to the Retina Service of Tohoku University Hospital. Intravitreal intervention and follow-up were both performed at this clinic.

Patients

The study comprised 25 eyes of 22 patients (eleven men and eleven women, mean age: 67.5 years) with retinal disease (DR group: 12 eyes of nine patients with DR; BRVO group: 13 eyes of 13 patients with BRVO) and macular edema.

Each patient provided informed consent for their participation in this study as well as for the treatments they received. The study was approved by the institutional review board of Tohoku University Graduate School of Medicine (Protocol No 2013-164; May 17, 2013). The research was conducted according to the provisions of the Declaration of Helsinki, 1995 (as revised in Edinburgh, 2000).[26,27]

Intervention

In all eyes, after instillation of topical anesthetic (0.4% oxybuprocaine hydrochloride; Benoxil), sterilization of the eyelid (10% povidone-iodine Swabstick), and instillation of 1.25% povidone-iodine (Isodine), 1.25 mg/0.05 mL of bevacizumab (Avastin) was injected into the vitreous cavity with a standard pars plana approach (3.5 mm posterior to the limbus) using a 30-gauge needle.

Measurement of clinical findings

We measured best-corrected visual acuity (BCVA) before, 1 week after, and 1 month after IVB. Similarly, we measured foveal thickness (FT) before, 1 week after, and 1 month after IVB. BCVA was measured with a logMAR chart (5 m) (LVC-10; NEITZ Instruments, Tokyo, Japan), and retinal thickness was measured with optical coherence tomography (OCT) (OCT3000; Carl Zeiss Meditec AG, Jena, Germany). The retinal thickness of the central fovea was defined as the distance between the inner limiting membrane and the retinal pigment epithelium, and was automatically calculated by the OCT3000 software. A macular thickness map was made with the OCT retinal mapping program from six radial scans intersecting at the fovea. The mean retinal thickness was calculated in nine regions: the 1,000 μm central area and the four quadrants of the inner and outer rings. FT was defined as the value of the 1,000 μm central area. Blood pressure and intraocular pressure (IOP) were measured after 10 minutes of rest.

Measurement using laser speckle flowgraphy

We measured MBR with the LSFG NAVI system (Softcare Co., Ltd., Fukutsu, Japan) before, 1 week after, and 1 month after IVB. The measurement conditions were kept constant as follows: angle of view, 21°; number of pixels measured, 750×360; and laser power, 1.37 mW. Determination of MBR was made with LSFG Analyzer software (version 3.0.47.0; Softcare Co., Fukutsu, Japan). We measured four regions: a selected retinal artery, a selected retinal vein, the optic nerve head (ONH), and the choroid. Measurements for the retinal artery and the retinal vein were taken from sites near the ONH (within 1.5 papilla

diameters). In patients with BRVOME, blood vessels in the quadrant containing the obstruction were not selected in order to avoid the influence of the hemorrhage. The mean number of samples was 1,013, 1,482.3, and 47,785.2 in the retinal artery, the retinal vein, and the ONH, respectively. Measurement of the choroid was performed in a square area (150×150 pixels; 19,479 samples) not containing retinal blood vessels, in a temporal location located one papilla diameter away from the ONH. Only a single measurement of each region was performed.

Statistical analysis

Analysis was done with Ekuseru-Toukei 2006 software (Social Survey Research Information Co., Ltd., Tokyo, Japan). The data are presented as mean ± standard deviation. The significance of the difference between pre- and post-IVB data was assessed with the Friedman test and Scheffe's paired comparison. We also used the Mann–Whitney *U* test to compare characteristics other than sex and optic media and clinical findings before and after IVB in the BRVO and DR groups. Sex and optic media were compared with Fisher's exact test. The Spearman correlation coefficient was used to determine the relationship between MBR and FT in the ONH. A *P*-value of less than 0.05 was considered to be statistically significant.

Results

A comparison of characteristics and findings before and after IVB in the BRVOME and DME groups is shown in Table 1. Before IVB, there were no significant differences in age, optic media, IOP, or FT between the two groups, but there were significant differences in sex distribution and visual acuity. After IVB, there was no difference in IOP between the two groups, but there was a significant difference in FT. FT in the BRVOME group was significantly lower than in the DME group 1 month post-IVB.

BCVA and FT before and after IVB are shown in Figures 1 and 2, respectively. MBR in the retinal artery, retinal vein, ONH, and choroid before and after IVB is shown in Figure 3. In the DME group, MBR changed significantly in all regions 1 week and 1 month after IVB (retinal artery, $P=0.02$; retinal vein, $P=0.04$; ONH, $P<0.001$; and choroid, $P=0.04$). In the BRVOME group, MBR did not change significantly 1 week or 1 month after IVB in any of the measured regions (retinal artery, $P=0.09$; retinal vein, $P=0.33$; ONH, $P=0.50$), except the choroid ($P=0.04$).

The relationship between FT and MBR in the ONH of the DME group is shown in Figure 4. Pre-IVB MBR in the ONH was not correlated with pre-IVB FT ($P=0.33$), but post-IVB MBR in the ONH was correlated with post-IVB FT ($R=-0.80$, $P=0.009$). Furthermore, pre-IVB MBR in the ONH was correlated with post-IVB FT ($R=-0.71$, $P=0.002$). The relationship between FT and MBR in the ONH of the BRVOME group is shown in Figure 5. There were no equivalent correlations in the ONH of the BRVOME group.

Representative eyes with DME and BRVOME are shown in Figures 6 and 7, respectively.

Complications arising from IVB, such as endophthalmitis, ocular hypertension, retinal detachment, and vitreous hemorrhage, did not occur in any of the patients in this study.

Table 1 Comparison of characteristics and findings before and after intravitreal injection of bevacizumab in groups with branch retinal vein occlusion and diabetic retinopathy

Group	BRVOME	DME	*P*-value
Number of eyes	13	12	
Age	71.0±9.6	63.8±9.2	0.0565[a]
Sex (M: F)	(4:9)	(7:2)	*0.0402[b]
Optic media (lens: pseudophakia)	(11:1)	(10:3)	0.3278[b]
BCVA (logMAR)			
Pre-IVB	0.8±0.26	0.41±0.21	**0.0016[a]
1 week post-IVB	0.64±0.4	0.49±0.23	0.3355[a]
1 month post-IVB	0.64±0.33	0.45±0.29	0.1245[a]
IOP (mmHg)			
Pre-IVB	13.6±2.4	12.8±1.5	0.2409[a]
1 week post-IVB	12.1±2.3	13.4±2.3	0.1818[a]
1 month post-IVB	12.9±2.1	12.6±2.2	0.8062[a]
Foveal thickness (μm)			
Pre-IVB	549.8±127.7	465.7±120.1	0.0727[a]
1 week post-IVB	327.5±110.1	396.8±116.1	0.2108[a]
1 month post-IVB	270.2±67.9	408.3±148.6	**0.0036[a]

Notes: [a]Mann–Whitney *U* test; [b]Fisher's exact test. *$P<0.05$; **$P<0.01$.
Abbreviations: BCVA, best-corrected visual acuity; BRVOME, branch retinal vein occlusion-associated macular edema; DME, diabetic macular edema; IOP, intraocular pressure; IVB, intravitreal bevacizumab; logMAR, logarithm of the minimum angle resolution; M, male; F, female.

Discussion

We set out to investigate the effect of IVB on the retina in DME and BRVOME patients, in particular its effect on ocular blood flow. We found that in BRVOME patients, there was no significant change in MBR in any of the areas measured in this study, with the exception of a significant decrease in the choroid. In the group of patients with DME, there was a significant decrease in MBR in all measured areas. Interestingly, however, we observed that pre-IVB MBR in the DME patients was significantly correlated with post-IVB FT; specifically, higher MBR before IVB was correlated with lower FT after IVB.